

LOCALIZATION OF PLASMA LAYERS IN THE IONOSPHERE BASED ON OBSERVING VARIATIONS IN THE PHASE AND AMPLITUDE OF RADIO WAVES ALONG THE SATELLITE-TO-SATELLITE PATH

A. G. Pavelyev,^{1*} J. Wickert,² and Y. Liou³

UDC 621.371

We propose a method for localization of layered structures in the ionosphere, which is based on simultaneous observations of time variations in the intensity and phase of radio waves along transionospheric paths. The method determines the position of the turning point, where the gradient of the refraction index is perpendicular to the ray trajectory and the influence of the layered structure on the parameters of radio waves is maximal. The layer position is estimated by analyzing the variations in the phase and intensity of radio waves in combination. The method was used to analyze the experimental data obtained by the radio occultation mission CHAMP. The position for inclined plasma layers was determined and the electron density distribution was found for the considered radio occultation sessions. The method was verified by measuring the turning point on the ray trajectory in a neutral gas in the atmosphere.

1. INTRODUCTION

Radio occultation (RO) experiments are currently performed on transionospheric satellite-to-satellite paths using coherent signals emitted by the navigation systems GPS (USA) and GLONASS (Russia). These experiments are aimed at studying physical properties of the atmosphere and ionosphere at different altitudes on the global scale including hardly accessible oceanic and polar regions [1, 2]. The method of RO experiments are based on the assumption about the global spherical symmetry of the atmosphere and ionosphere with the center, which coincides approximately with the center of the Earth. Under this assumption, the altitude of the layered structure coincides with the altitude of the perigee of the ray trajectory [1–3]. Horizontal gradients of the refraction ratio cause inclinations of plasma layers in the ionosphere and result in changes in the position of the spherical-symmetry center [4]. As a result, significant variations in the amplitude and phase of RO signals are frequently observed at altitudes of the ray-trajectory perigee ranging from 40 to 80 km, in which the expected contribution of the neutral gas or electron density to the variations in the RO signal is negligibly small. Earlier, the authors of [5] and [6] proposed a radio holography back-propagation method for localization of plasma inhomogeneities in the ionosphere. Within the framework of this method, the electromagnetic field in the space between a transmitter and a receiver is retrieved using the radio hologram recorded at a certain interval of the trajectory of a low-orbit satellite. The coordinates of inhomogeneities are determined from the position of the minimum of amplitude variations in the retrieved field [5, 6]. This paper proposes a simpler approach which can be used to determine the position and estimate the parameters of inclined plasma layers in the ionosphere along satellite-to-satellite paths.

* pvlv@ms.ire.rssi.ru

¹ Institute of Radioengineering and Electronics of the Russian Academy of Sciences, Fryazino, Moscow Region, Russia, ² GeoForschungsZentrum, Potsdam, Germany, ³ Center for Remote Sensing and Space Research, National Central University, Taiwan, China. Translated from *Izvestiya Vysshikh Uchebnykh Zavedenii, Radiofizika*, Vol. 51, No. 1, pp. 1–9, January 2008. Original article submitted July 19, 2006; accepted February 1, 2007.

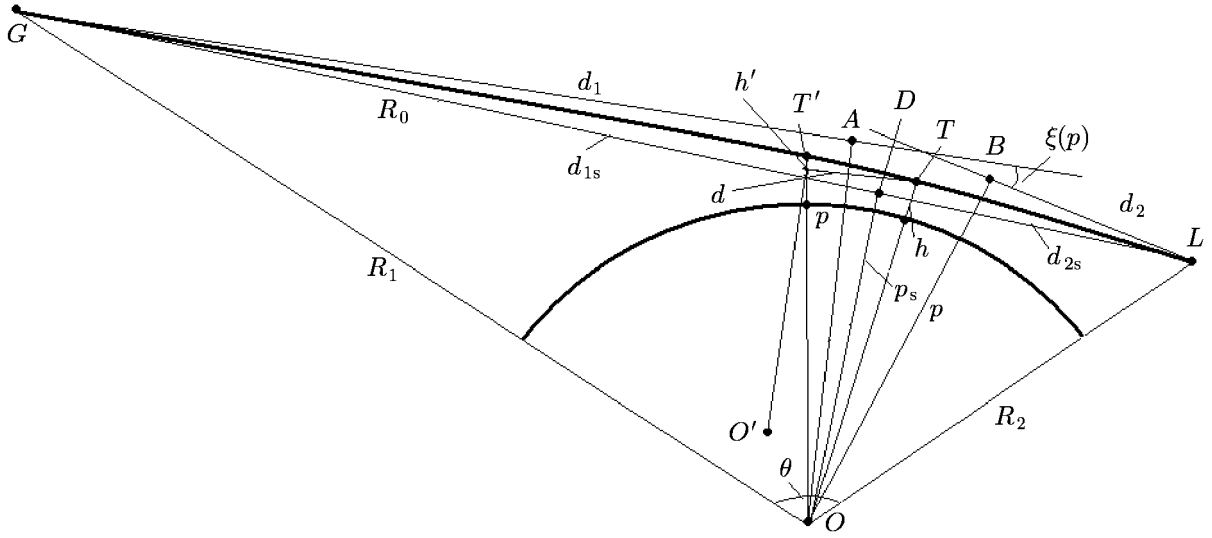


Fig. 1. Scheme of radio probing on the satellite-to-satellite path.

2. BASIC RELATIONSHIPS

The scheme of the radio occultation (RO) experiment using radio signals emitted by a GPS navigation system satellite on the transionospheric satellite-to-satellite path is shown in Fig. 1. The point O is the center of spherical symmetry of the atmosphere and ionosphere of the Earth. Radio waves emitted by the GPS satellite (point G) reach the receiver on board a low-orbit satellite (point L) having passed along the ray GTL , where T is the turning point in the atmosphere. At point T , the gradient of the refraction ratio $N(h)$ is perpendicular to the ray trajectory GTL (Fig. 1). The RO method supposes that point T coincides with the perigee of the RO ray (see, e.g., [3]) and, therefore, the altitude of the ray trajectory over the Earth's surface is minimal at point T . The projection of point T on the Earth's surface determines the geographic coordinates of the studied region.

The records of RO signals along the orbit of the low-orbit satellite L at two GPS frequencies, $f_1 = 1575.42$ MHz and $f_2 = 1227.6$ MHz, contain two amplitudes, $A_1(t)$ and $A_2(t)$, and two phases, $\Phi_1(t)$ and $\Phi_2(t)$, of the RO signal as a function of time with an interval between successive readouts being equal to 0.02 s. The vertical velocity of the radio occultation beam v_\perp is equal to approximately 2 km/s. The value of v_\perp is significantly higher than the velocities of motion of the layered structures in the ionosphere and atmosphere. Consequently, the RO signal contains a nearly instantaneous snapshot of the near-Earth space in the studied region. The length of the phase path $\Phi(p)$ is measured in radio occultation experiments as a difference of the phase path along the actual ray trajectory GTL (Fig. 1) and the phase path along the line-of-sight GDL , where D is the projection of the spherical-symmetry center O on the straight line GL (Fig. 1). The refraction attenuation $X(p)$ is equal to the intensity of the radio waves having passed along the trajectory GTL normalized to radio wave intensity and calculated for the path GDL under the assumption about propagation in free space. In the case of spherical symmetry of the ionosphere and the atmosphere, the length of the phase path $\Phi(p)$ and the refraction attenuation of radio waves $X(p)$ depend only on the impact parameter p , which is constant along the ray trajectory GTL (Fig. 1), and are determined using relationships [7, 8]

$$\Phi(p) = L(p) + \kappa(p) - R_0, \quad L(p) = d_1 + d_2 + p\xi(p), \quad (1)$$

$$X(p) = pR_0^2 [R_1R_2d_1d_2 \sin \theta |\partial\theta/\partial p|]^{-1}, \quad (2)$$

$$\partial\theta/\partial p = d\xi/dp - (1/d_1 + 1/d_2), \quad (3)$$

where $\kappa(p)$ is the main refraction part of the phase path, $\xi(p) = -d\kappa(p)/dp$ is the refraction angle of radio

waves, $\theta(p)$ is the central angle, p and p_s are impact parameters of the beam trajectory GTL and the line-of-sight GDL , respectively, R_0 , R_1 and R_2 are the distances GDL , OG and OL , respectively, and $L(p)$ is the distance $GABL$ equal to the sum of the distances d_1 (GA), d_2 (BL) and the circular arc AB $p\xi(p)$ (Fig. 1). The distance d_2 is approximately equal to the distances TL and DL due to the smallness of the refraction effect in the ionosphere at the frequencies of the GPS navigation system. In the case of $|p - p_s| \ll p_s$, we have

$$d\Phi(p)/dt \approx (p - p_s) (dp_s/dt) (\partial\theta/\partial p_s), \quad (4)$$

$$\partial\theta/\partial p_s = -(1/d_{1s} + 1/d_{2s}), \quad (5)$$

where d_{1s} and d_{2s} are the distances GD and DL , respectively (Fig. 1). An approximate formula for the second time derivative of $\Phi(p)$ can be obtained from Eq. (4) in the case

$$|(p - p_s) d(dp_s/dt \partial\theta/\partial p_s)/dt| \ll |(dp/dt - dp_s/dt) dp_s/dt \partial\theta/\partial p_s| \quad (6)$$

and is written as

$$d^2\Phi(p)/dt^2 \approx (dp/dt - dp_s/dt) dp_s/dt \partial\theta/\partial p_s. \quad (7)$$

Condition (6) and Eq. (7) are fulfilled for slow changes in the values $p_s(t)$ and dp_s/dt during radio occultation measurements. From the approximate equality

$$dp/dt - dp_s/dt \approx (X(t) - 1) dp_s/dt, \quad (8)$$

which was obtained earlier in [7], and Eq. (7) one can obtain

$$1 - X(t) = ma, \quad a = d^2\Phi(t)/dt^2, \quad (9)$$

$$m = q/(dp_s/dt)^2, \quad (10)$$

$$q = d_{1s}d_{2s}/(d_{1s} + d_{2s}) = d_{1s}d_{2s}/R_0. \quad (11)$$

Equation (9) determines the equivalence of the variation $a = d^2\Phi(t)/dt^2$ in the acceleration of the phase to the time derivative $F_d = d\Phi(t)/dt$ of the Doppler frequency and the refraction attenuation $X(t)$. The parameters m and dp_s/dt can be determined from the orbital data when the assumption about the spherical symmetry of the atmosphere and the ionosphere with the center O is fulfilled, since the position of the projection D of the point O on the line-of-sight GDL is known (Fig. 1):

$$dp_s/dt = v + (w - v) d_{2s}/R_0, \quad (12)$$

where v and w are the components of the velocities of the navigation satellite and low-orbit satellite, respectively, which are perpendicular to the straight line GL within the plane GOL . Equations (9)–(12) can be used to determine the distance d_{2s} (LD) from the simultaneous measurements of the variations in the phase and intensity of the radio waves:

$$d_{2s} = 2(v^2 m) [1 + 2\beta(v/w - 1) + (1 - 4\beta v/w)^{1/2}]^{-1}, \quad \beta = mv^2/R_0. \quad (13)$$

Horizontal gradients in the ionosphere can displace the center O of the spherical symmetry to the point O' (Fig. 1). In this case, the turning point T will be displaced away from the perigee along the ray trajectory to the point T' , which will result in changes in the parameter m . In this case, Eqs. (9)–(13) can be used within the approximation of the local spherical symmetry with the new center O' under the following assumptions: 1) absence of multipath propagation and 2) fulfillment of inequalities (6). In the three-dimensional case, the new center O' can be located out of the plane GOL and to determine the parameter m , it is necessary to take into account the dihedral angle between the planes GLO and GLO' . The possibility of localization of

plasma layers in the presence of significant gradients in the azimuthal direction which is perpendicular to the plane *GLO*, requires additional consideration being the subject of further studies.

If the value of the parameter m is determined from the experimental data, there is a possibility for determining the deviation d of the point t relative to the perigee of the RO beam. In this case, we assume that m is a slowly changing function of time. If the noise level is low, then the parameter m can be determined from Eq. (9):

$$m = [1 - X(t)]/a. \quad (14)$$

In the presence of noise, the value of the ratio $m(t_k)$ at the time instant t_k can be obtained by averaging the squares of variations in the phase acceleration and refraction attenuation from the formula

$$m(t_k) = \left\{ \frac{\sum_{i=k-M}^{i=k+M} [X(t_i) - 1]^2}{\sum_{i=k-M}^{i=k+M} [a(t_i)]^2} \right\}^{1/2}, \quad (15)$$

where $2M$ is the number of samples used for averaging. Equation (15) can be used under the condition of full correlation of the refraction attenuation and phase acceleration, i.e., when Eq. (9) is fulfilled. Under real conditions, there are different sources of variations in the amplitude and phase of the RO signal (turbulence, multipath propagation, etc.), for which Eq. (9) can be violated. Equation (9) is fulfilled for the amplitude and phase variations corresponding to inclined layers. For the inclined layers, the parameter m can be determined from the correlation relationship:

$$m(t_k) = \frac{\sum_{i=k-M}^{i=k+M} [1 - X(t_i)] a(t_i)}{\sum_{i=k-M}^{i=k+M} [a(t_i)]^2}. \quad (16)$$

Equations (15) and (16) determine the upper and lower boundaries, respectively, in the determination of the parameter m from the variations in the intensity and phase of the RO signal. Having determined the parameter m , one can estimate the upper and lower boundaries for the distance $d = d'_2 - d_2 = d'_2 - (R_2^2 - p^2)^{1/2}$, where d'_2 is the distance between the projection of the displaced centre of the spherical symmetry O' on the line *GDL* and the low-orbit satellite L (Fig. 1) from Eqs. (9)–(13). This distance is approximately equal to the distance $T'L$.

3. ANALYSIS OF THE DATA OF RADIO OCCULTATION EXPERIMENTS ON THE CHAMP SATELLITE

The RO mission on the “CHallenging Mini Payload” (CHAMP) satellite, which used the signals from the GPS satellites, was described in [9]. To check the fulfillment of Eq. (9), we will consider the data obtained in Session No. 0069 in September 21, 2003, at 05:33 LT in the region having the geographic coordinates 40.4°N and 19.6°W (Fig. 2). In Fig. 2a, the changes in the phase, which are related to the influence of the atmosphere and the ionosphere, are presented for the frequencies f_1 and f_2 (curves 1 and 2, respectively), depending on the altitude h of the perigee of the beam trajectory *GTL* (Fig. 1). For the altitudes above 45 km, the changes in the phase path are given in meters, for those below 45 km, in kilometers. For the sake of comparison, the curves in Fig. 2a are displaced. Curve 3 in Fig. 2a was obtained from phase paths at the frequencies f_1 and f_2 by means of ionospheric correction. Curve 3 shows the part of the phase path corresponding to the neutral atmosphere. It is displaced to 300 m for the sake of comparison with curve 4 calculated for the standard model of the neutral atmosphere. At the altitudes above 45 km, the variations in the phase path are illustrated by curves 5–8. Curves 5 and 6 describe the contribution of the standard neutral atmosphere calculated by means of the atmospheric model [10] and the ionospheric correction of the experimental data [3], respectively. According to curves 5 and 6, the contribution of the neutral atmosphere changes from 20 cm at an altitude of 45 km to 2 cm at an altitude of 60 km. Curves 7 and 8 correspond to the experimental dependences of the phase path on the altitude at the frequencies f_1 and f_2 . For the

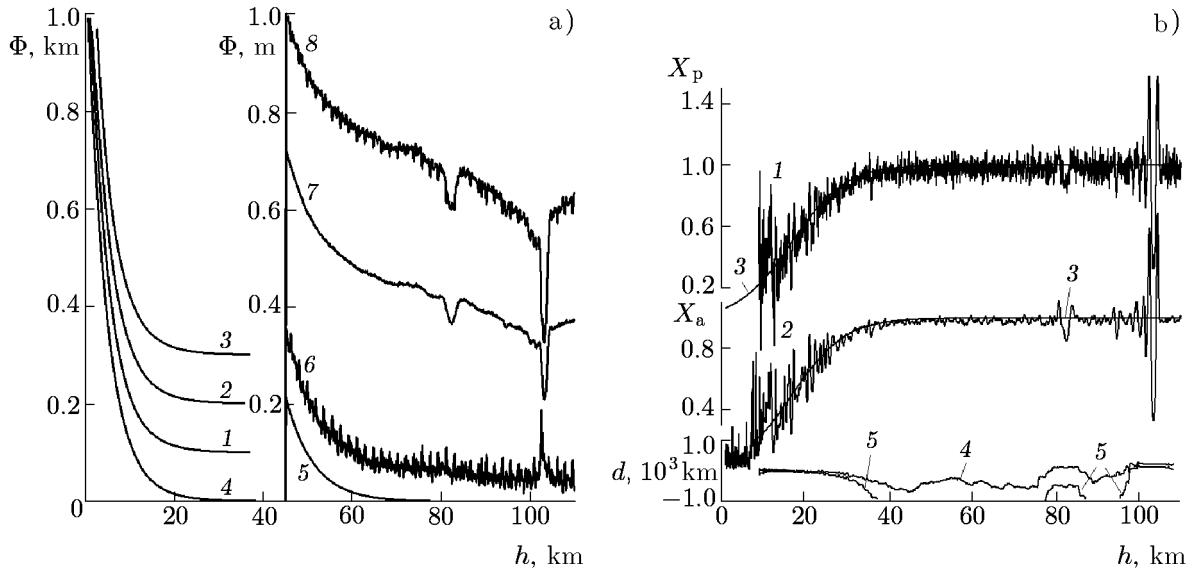


Fig. 2. (a) Changes in the phase path at the frequencies f_1 and f_2 (curves 1 and 2), which are connected with the influence of the ionosphere and the atmosphere depending on the height of the perigee of the satellite-to-satellite ray trajectory. For comparison, curves 1 and 2 are displaced by 100 and 200 m, respectively. Curve 3 was obtained from the phase paths at the frequencies f_1 and f_2 by means of ionospheric correction. Curve 3 shows the part of the phase path corresponding to the neutral atmosphere and is displaced by 300 m as compared with curve 4 calculated for the standard atmospheric model. Curves 1–4 show the changes in the phase path at the altitudes below 45 km. At the altitudes above 45 km, the variations in the phase path are characterized by curves 5–8. Curves 5 and 6 describe the contribution of the standard neutral atmosphere calculated by using the atmospheric model and the ionospheric correction of the experimental data, respectively. Curves 7 and 8 correspond to the experimental dependences of the phase path on the altitude at the frequencies f_1 and f_2 . For the sake of comparison, curves 6, 7, and 8 are displaced relative to curve 5 by 5, 30, and 50 cm, respectively. (b) Comparison of the variations in the phase acceleration recalculated into the refraction attenuation X_p (curve 1), and of the refraction attenuation X_a (curve 2) determined from the intensity of the RO signal at the first harmonic of the GPS navigation system.

sake of comparison, curves 6, 7, and 8 are displaced relative to curve 5 by 5, 30, and 50 cm, respectively. According to Fig. 2a, the influence of the ionosphere on the changes in the phase path when the altitude of the perigee of the beam trajectory is above 45 km, exceed significantly the contribution of the neutral ionosphere (curves 7 and 8), and the variations in the phase path at the second frequency (curve 8) are more significant. Note that during this session, the measurements at the second frequency are complicated by the interference in the form of periodic peaks. This interference complicates the measurements of the contribution of the neutral atmosphere significantly, which are performed by using the ionospheric correction by the method of linear combination of the phase paths at the first and second frequencies [3] (curve 6). The phase path at the first frequency (curve 7) was measured with highest quality. These measurements were used in what follows for the further analysis. At the altitudes below 45 km, the influence of the neutral atmosphere is dominant (curves 1–4 in Fig. 2a), and the contribution of the neutral atmosphere into the phase path reaches 1 km near the Earth's surface. Curves 1 and 2 in Fig. 2b describe the variations in the refraction attenuations calculated from the phase acceleration and intensity of the RO signal at the frequency f_1 , respectively. Smooth curves 3 correspond to the results of modeling of the refraction attenuation for the exponential model of the altitude dependence of the refraction index for the neutral atmosphere [10]. Curves 4 and 5 in Fig. 2b describe the displacement d of the point T relative to the perigee of the ray path. The value d was calculated from Eqs. (9)–(13) by using Eq. (15) (curve 4) and Eq. (16) (curve 5). In Fig. 2b, one can see a significant correlation between the phase acceleration and the refraction attenuation in the

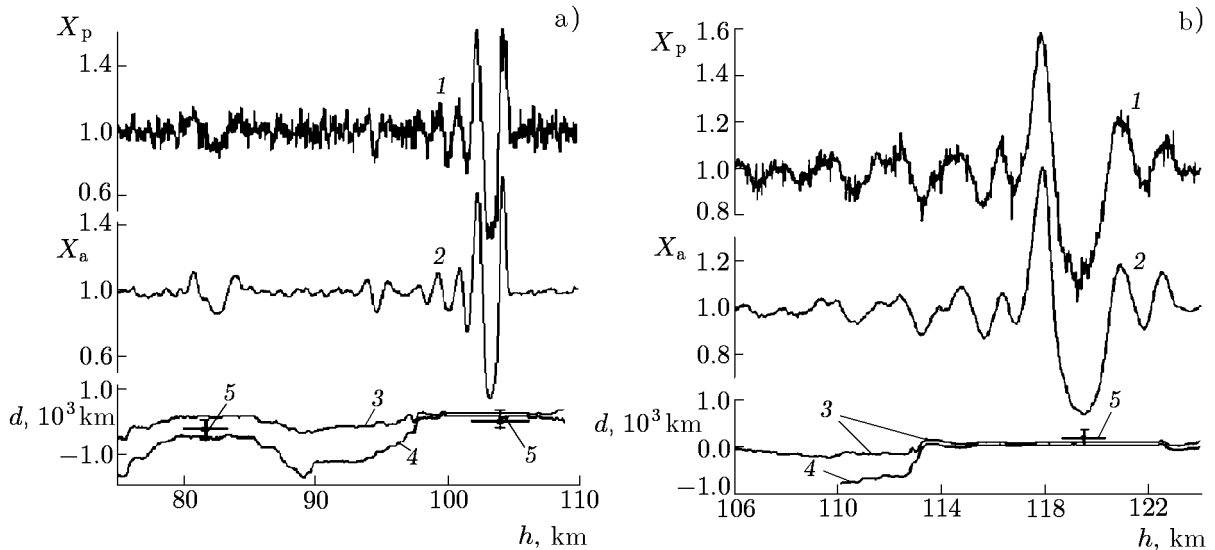


Fig. 3. Comparison of phase acceleration variations a converted into the refraction attenuation X_p , and of the refraction attenuation X_a found from the amplitude data at the first GPS frequency f_1 (curves 1 and 2), and the results of determining the displacement d of the turning point T from the perigee of the RO ray (curves 3 and 4). The data relate to sessions No. 0069 (panel a) and No. 0169 (panel b). Vertical and horizontal intervals 5 correspond to the estimation of the displacement d obtained by the back-propagation method.

altitude interval 10–30 km, where curves 4 and 5 practically coincide and the point T is at the perigee of the ray trajectory GTL . The displacement d in the above-mentioned altitude interval ranges from 100 to 200 km, which corresponds to the theoretical estimation of the horizontal resolution of the RO method. This correlation confirms that Eq. (9) is fulfilled and the considered method can be used for the case of the neutral atmosphere. In the intervals of the perigee of the ray trajectory 35–80 km and 88–96 km, curves 4 and 5 do not coincide, which corresponds to a different mechanism of phase acceleration variations a and refraction attenuation of radio waves (Fig. 2b). The correlation between the variations in the phase acceleration and the refraction attenuation of radio waves exists at altitudes of 80–86 km and 98–106 km (Fig. 2b). This connection may occur due to the influence of sporadic E_s layers in the ionosphere (curves 1 and 2 in Fig. 2b).

Variations in the RO signal due to the influence of sporadic E_s layers are considered in detail in Fig. 3 using as an example the data obtained in two sessions of the CHAMP mission: (a) No. 0069, September 21, 2003 (coordinates 40.4°N, 19.6°W), and No. 0169, July 05, 2003 (coordinates 29.4°S, 232.9°W). In session No. 0069, two sporadic E_s layers are observable (Fig. 3a) with the centers at altitudes of 82.5 km and 103.5 km of the perigee of the RO ray. A response of the sporadic E_s layers is frequently observed in RO experiments at altitudes ranging from 80 to 90 km of the perigee of the RO ray. The authors of [11] think that this altitude range corresponds to the real altitude of the sporadic E_s layers above the Earth's surface. However, this altitude range is unusual for the sporadic E_s layers [12] and contradicts the main mechanisms of their formation. Favorable conditions for the formation of the sporadic E_s layers exist at altitudes 100–130 km [12]. As the altitude decreases, the collision rate increases sharply, which is the main obstacle for the formation of the sporadic E_s layers below 90 km. The authors of [4] made an assumption that the variations in the amplitude and phase of the RO signal observed in the altitude range from 40 to 90 km correspond to the inclined layers of plasma in the ionosphere, which are displaced vertically and horizontally relative to the perigee of the ray trajectory GTL . The value of the displacement d can be estimated using curves 3 and 4 (Fig. 3a). For example, an estimation using curves 4 calculated from correlation relationship (16) yields $d \approx -530$ km. For the sake of comparison, the displacement d was also estimated by the back-propagation method, the details of which are described in [5, 6]. Curves 3 and 4, as well as vertical and horizontal intervals of straight lines 5 in Fig. 3 correspond to the estimation of the displacement d by the

proposed method and the method of back-propagation of radio waves [5, 6]. As follows from an analysis of the data in Fig. 3, the considered method and the back-propagation method yield coinciding results within the accuracy of measurements. Note that the back-propagation method is significantly more complicated than the proposed method. According to Fig. 3, the first sporadic E_s layer is localized on the ray trajectory between the points D and L (Fig. 1) at a distance of about 550 km relative to the perigee of the RO ray.

To determine the altitude $h'(T')$ and the inclination δ of the plasma layer in the ionosphere from the known displacement d , one can use the relationship [4]

$$h'(T') = h + [2d(r_0 + h)]^{1/2}, \quad \delta = d/r_0, \quad (17)$$

where r_0 is the Earth's radius. The inclination of the first layer to the local horizon is of the order of 8.9° , and the adjusted altitude of the layer above the Earth's surface changes in the range from 96 km to 98 km (Fig. 3a).

The second sporadic E_s layer is situated practically in the perigee of the PO beam at an altitude of about 103 km since curves 3 and 4 yield the same value of d , which is close to zero (Fig. 3a). In session No. 0169, the center of the sporadic E_s layer is localized at an altitude of 119.5 km, and is almost coincident with the perigee of the RO ray since the distance d (curves 3 and 4 in Fig. 3b) is close to zero within the accuracy of measurements. An estimation of the measurement error for d as the difference of curves 3 and 4 in Fig. 3 yields a value ranging from 30 to 100 km. Therefore, the proposed method is promising for localization of the sporadic E_s layers and, probably, inclined plasma layers of another origin in the ionosphere.

4. ESTIMATION OF PLASMA PARAMETERS

To estimate the plasma density in inclined ionospheric layers, one has to apply the method for solving of the inverse problem described earlier in [8]. In accordance with this method, the vertical gradient of the refraction ratio and the altitude profile of the electron density are retrieved based on variations in the RO signal amplitude. Then, after integration, the vertical profile of electron density variations is found. The results of retrieving the variations $\Delta N_e(h)$ in the electron density and its gradient $dN_e(h)/dh$ based on the amplitude of the RO signal variations are shown in Fig. 4 for sessions Nos. 0069 and 0169 (panels *a* and *b*, respectively). Variations in the phase acceleration a and in the refraction attenuation X are shown by curves 1 and 2 in Fig. 4. Curves 3 and 4 in Fig. 4 describe the retrieved variations $\Delta N_e(h)$ and $dN_e(h)/dh$ as functions of the adjusted (by means of Eq. (16)) altitude h . Curves 1 and 2 are well agreed, especially in session No. 0169, where they are nearly coincident (Fig. 4b). Actually, it is another example of the fulfillment of Eq. (9) for the case of the sporadic E_s layer. According to Fig. 4, the perturbations $\Delta N_e(h)$ of the electron density lie within the range $\pm(5-25) \cdot 10^9 \text{ m}^{-3}$, and the vertical gradient $dN_e(h)/dh$, in the interval $\pm(20-50) \cdot 10^9 \text{ m}^{-3}/\text{km}$. The above-mentioned values of the electron density variations and its vertical gradients in the altitude range 90–124 km correspond to the values characteristic of the sporadic E_s layer in the ionosphere (see, e.g., [12]).

5. CONCLUSIONS

The new method based on the combined analysis of variations in the phase acceleration and the refraction attenuation is promising for the localization of layered structures in the near-Earth space. Its efficiency is illustrated by means of analysis of the experimental data recorded by the CHAMP satellite. In the future, it is desirable to compare the developed method with the results of observations from ground-based ionosondes. The presented method and other new methods allow obtaining a growing bulk of data about plasma structures and natural processes in the ionosphere, and their connection with the processes in the magnetosphere and interplanetary space by analyzing the data of the satellite missions GPS/MET, CHAMP, SAC-G, GRACE, and FORMOSAT-3, which functioned in the past and are functioning now.

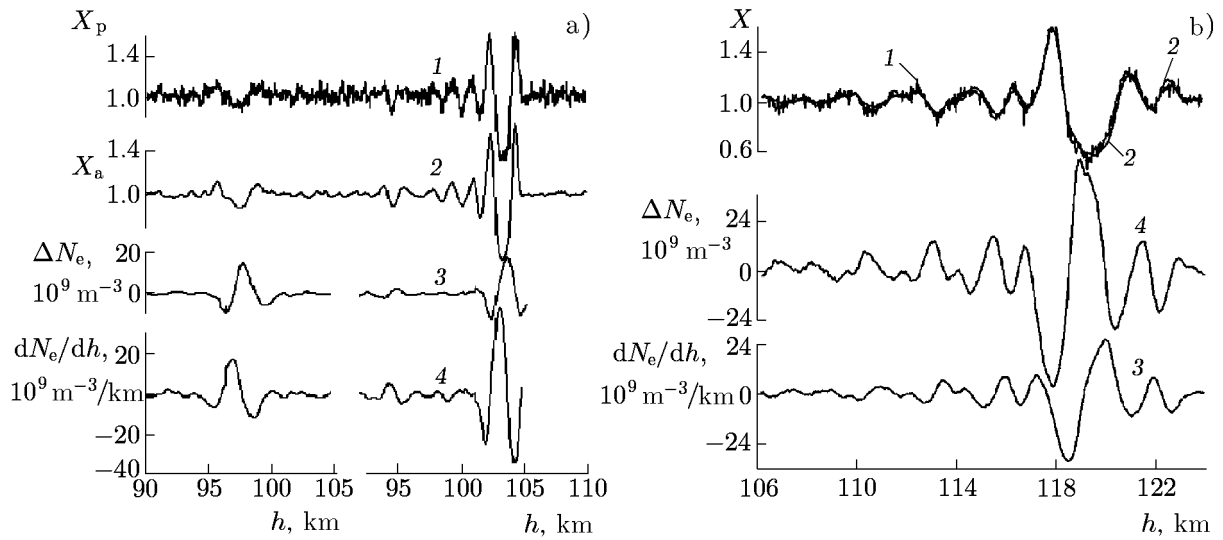


Fig. 4. Comparison of the phase acceleration variations a converted into the refraction attenuation X_p and the refraction attenuation X_a found from the amplitude data at the first GPS frequency f_1 (curves 1 and 2), and the restored variations in the electron density and its vertical gradients as functions of the adjusted altitude in the ionosphere. The data correspond to session No. 0069 (panel *a*) and No. 0169 (panel *b*). The adjusted altitude of the weakly ionized ionospheric layer (with the maximum near 96 km) is little different from the altitude of the intense layer situated at an altitude of about 10 km. This is emphasized by the introduction of two horizontal axes in panel *a*.

The authors are grateful to the GeoForschungsZentrum (Potsdam, Germany) for the possibility to use the experimental data of the CHAMP satellite. This work was supported by the National Scientific Council of Taiwan (project No. NSC 94-2811-M-008-055), the Russian Foundation for Basic Research (RFBR) (project No. 06-002-17071), and the programs of the Russian Academy of Sciences OFN-16 and OFN-17.

REFERENCES

1. O. I. Yakovlev, *Space Radiophysics* [in Russian], RFBR, Moscow (1998).
2. E. R. Kursinski, G. A. Hajj, J. T. Schofield, et al., *J. Geophys. Res.*, **102**, 23429 (1997).
3. G. A. Hajj, E. R. Kursinski, L. J. Romans, et al., *J. Atmos. Sol. Terr. Phys.*, **64**, 451 (2002).
4. J. Wickert, A. G. Pavelyev, Y. A. Liou, et al., *Geophys. Res. Lett.*, **31**, No. 24, L24801 (2004).
5. M. E. Gorbunov, A. S. Gurvich, and A. V. Shmakov, *Int. J. Remote Sensing*, **23**, No. 4, 675 (2002).
6. S. V. Sokolovskiy, W. Schreiner, C. Rocken, and D. Hunt, *Geophys. Res. Lett.*, **29**, No. 3, 621 (2002).
7. A. G. Pavelyev, Y. A. Liou, and J. Wickert, *Radio Sci.*, **39**, No. 4, 4011 (2004).
8. Y. A. Liou, A. G. Pavelyev, J. Wickert, et al., *GPS Solut.*, **9**, 122 (2005).
9. J. Wickert, Ch. Reigber, G. Beyerle, et al., *Geophys. Res. Lett.*, **28**, 3263 (2001).
10. A. G. Pavelyev, A. V. Volkov, A. I. Zakharov, et al., *Acta Astronautica*, **39**, No. 9-12, 721 (1996).
11. D. L. Wu, O. A. Chi, G. A. Hajj, et al., *J. Geophys. Res.*, **110**, Art. no. A01306 (2005).
12. M. C. Kelly, *The Earth's Ionosphere: Int. Geophys. Ser.*, **43**, Elsevier, New York, 1989.